Developmental Cell *11*, 711–722, November, 2006 ©2006 Elsevier Inc. DOI 10.1016/j.devcel.2006.09.003

Zac1 Regulates an Imprinted Gene Network Critically Involved in the Control of Embryonic Growth

Annie Varrault,[1] Charlotte Gueydan,[1] Annie Delalbre,[1] Anja Bellmann,[1] Souheir Houssami,[1] Cindy Aknin,[1,2] Dany Severac,[1,2] Laetitia Chotard,[1] Malik Kahli,[1] Anne Le Digarcher,[1] Paul Pavlidis,[3,4] and Laurent Journot[1,2,*]

[1] Institut de Génomique Fonctionnelle
CNRS-UMR5203
INSERM-U661
Université Montpellier 1
Université Montpellier 2
Montpellier, F-34094
France

[2] Génopole Montpellier
Montpellier, F-34094
France

[3] Columbia Genome Center
College of Physician and Surgeons and
Department of Biomedical Informatics
Columbia University
New York, New York 10032

Summary

Genomic imprinting is an epigenetic mechanism of regulation that restrains the expression of a small subset of mammalian genes to one parental allele. The reason for the targeting of these ~80 genes by imprinting remains uncertain. We show that inactivation of the maternally repressed *Zac1* transcription factor results in intrauterine growth restriction, altered bone formation, and neonatal lethality. A meta-analysis of microarray data reveals that *Zac1* is a member of a network of coregulated genes comprising other imprinted genes involved in the control of embryonic growth. Zac1 alters the expression of several of these imprinted genes, including *Igf2*, *H19*, *Cdkn1c*, and *Dlk1*, and it directly regulates the *Igf2*/*H19* locus through binding to a shared enhancer. Accordingly, these data identify a network of imprinted genes, including *Zac1*, which controls embryonic growth and which may be the basis for the implementation of a common mechanism of gene regulation during mammalian evolution.

Introduction

Since the discovery of mammalian genomic imprinting in the mid 1980s (Cattanach and Kirk, 1985; McGrath and Solter, 1981; Surani et al., 1984), this form of epigenetic regulation has been the focus of extensive investigations (Constancia et al., 2004; Reik and Lewis, 2005). The mechanisms underlying parental origin-specific expression of several imprinted genes are now well understood (Delaval and Feil, 2004; Verona et al., 2003). The drive for the selection of genomic imprinting during mammalian evolution was formalized in the "parental conflict" or "kinship" theory (Moore and Haig, 1991; Wilkins and Haig, 2003). Presently, imprinting is understood as a mechanism aimed at controlling the amount of maternal resources allocated to the offspring from conception to weaning (Constancia et al., 2004). In contrast, fewer studies describe the biological function(s) carried out by imprinted genes. These genes are members of various gene families, and the corresponding proteins have diverse biochemical activities (Tycko and Morison, 2002), indicating that imprinting does not target a specific biochemical process. Conversely, a recurrent theme in the biology of imprinted genes is the control of embryonic development. Alteration of imprinted loci is consistently associated with developmental disorders in humans. Moreover, analysis of gain- and loss-of-function mouse mutants indicates that a number of imprinted genes are critically involved in the control of embryonic growth, either directly or by modulating the transport of nutrients across the placenta. At least two imprinted genes, *Mest*/*Peg1* and *Peg3*/*Pw1*, are additionally involved in controlling the quality of care that a mouse mother directs toward her offspring (Lefebvre et al., 1998; Li et al., 1999), and *GnasXL* is required for postnatal adaptation to feeding (Plagge et al., 2004). The number and identity of imprinted genes involved in each of these processes, and the underlying gene networks, remain ill defined at the moment.

Genomic imprinting of mouse *Zac1*, as well as its human ortholog *ZAC*/*LOT1*/*PLAGL1*, results in paternal-specific expression of the gene (Kamiya et al., 2000; Piras et al., 2000), which encodes a zinc finger transcription factor inducing apoptosis and cell-cycle arrest (Spengler et al., 1997; Varrault et al., 1998). Loss of *ZAC* expression is frequently observed in various neoplasms such as breast tumors (Bilanges et al., 1999), ovary tumors (Cvetkovic et al., 2004), nonfunctioning pituitary tumors (Pagotto et al., 2000), head and neck tumors (Koy et al., 2004), and basal cell carcinomas (Basyuk et al., 2005). Indeed, a tumor suppressor gene is known to reside on 6q24-q25, close to the *ZAC* locus. Furthermore, gain of *ZAC* function through biallelic expression, duplication of the paternal allele, or isodisomy of the paternal chromosome 6 is associated with transient neonatal diabetes mellitus (TNDM) (Gardner et al., 2000; Kamiya et al., 2000), a genetic disease resulting in defective development of the pancreas (Ma et al., 2004). Because *Zac1* displays abundant, albeit regionally restricted, expression during development (Valente and Auladell, 2001), we sought for a role for this imprinted gene in the control of embryonic development and inactivated the gene by homologous recombination.

Results

Generation of *Zac1*-Deficient Mice

To investigate a role for *Zac1* during embryonic development, we inactivated *Zac1* by homologous recombination in embryonic stem (ES) cells. We targeted the region

*Correspondence: laurent.journot@igf.cnrs.fr
[4] Present address: Bioinformatics Centre and Department of Psychiatry, University of British Columbia, Vancouver, British Columbia V6T 1Z4, Canada.

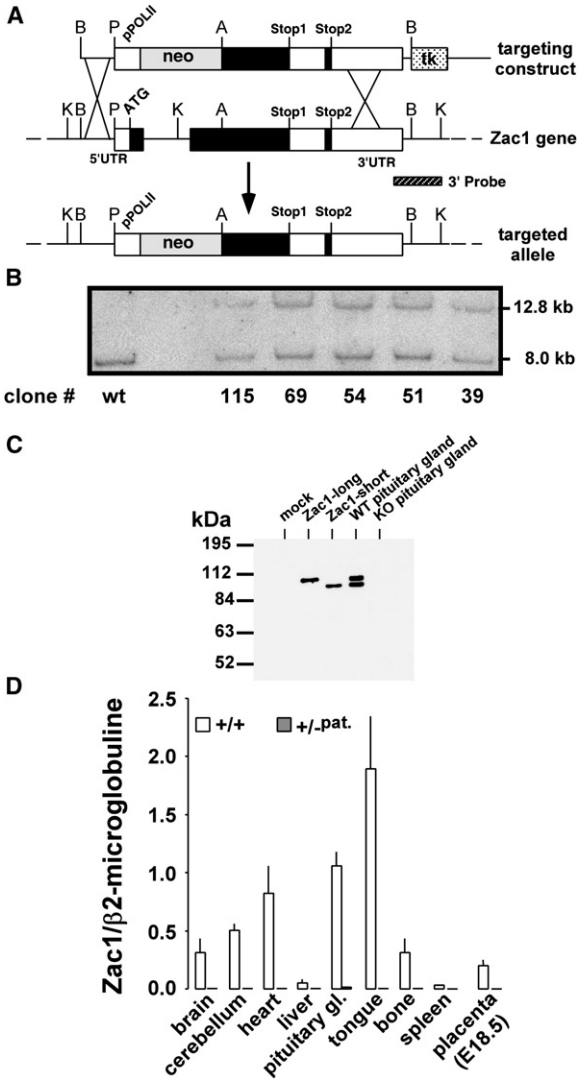

Figure 1. Targeted Disruption of *Zac1* Gene

(A) Structure of the targeting construct and of the mouse wild-type and knockout alleles. The coding region (black boxes) is within the two last exons (boxes) of *Zac1*. A *Pst*I (P)-*Ava*I (A) genomic fragment comprising the translation initiation site (ATG) and the entire zinc finger domain was replaced by a neomycin-resistance cDNA (neo) under the control of the polymerase II promoter (pPOLII). The translation termination sites (Stop1, Stop2) resulting from alternative splicing of the mRNA are indicated (Spengler et al., 1997). A PCR fragment downstream of the 3′ Bgl II (B) restriction site was used as a 3′ probe.

(B) Southern blot analysis of G418- and gancyclovir-resistant ES clones. Genomic DNA was prepared from the indicated ES clones, digested with *Kpn*I, run on an agarose gel, blotted to a nylon membrane, and probed with a radioactively labeled 3′ probe. Due to the replacement of a genomic sequence containing a *Kpn*I site by the neo cassette, the labeled band shifted from 8 kb (wt allele) to 12.8 kb (knockout allele).

(C) The absence of Zac1 protein in knockout animals was verified by western blotting. Total protein lysates were prepared from wild-type and $Zac1^{-/-}$ pituitary glands, run on a polyacrylamide gel, blotted onto a nitrocellulose membrane, and probed with a rabbit antiserum raised against bacterially produced GST-Zac1 fusion protein. The wild-type lysate displayed two immunoreactive bands corresponding to the two Zac1 isoforms arising from alternative splicing, as indicated by bands recognized by the antiserum in lysates from LLC-PK1 cells transfected with cDNAs encoding each of the isoforms. The knockout lysate does not display any immunoreactive bands, despite the fact that the antiserum recognizes a region of the protein not disrupted in the knockout allele.

(D) Expression of *Zac1* in P1 tissues and E18.5 placentas was assessed by real-time RT-PCR. No $Zac1^{+/-pat.}$ tissue exhibited *Zac1* expression, except the pituitary gland, which showed a very faint *Zac1* signal, i.e., 1.1% of the wild-type signal. Data are mean ± SD of three independent reverse transcription reactions.

encoding the N-terminal zinc finger domain by deleting the first and the 5′ part of the second coding exons (Figure 1A). G418- and gancyclovir-resistant clones were screened for homologous recombination with 3′ (Figure 1B) and 5′ (data not shown) probes. The absence of random integration was verified with a Neo probe (data not shown). The positive clones were microinjected into 3.5 day C57BL/6 blastocysts to generate chimerical animals. Male chimeras were mated to C57BL/6 females to produce *Zac1* heterozygotes. The F1 heterozygotes were backcrossed to C57BL/6 and CBA mice for more than ten generations, and the study was performed with animals >N10. Intercrosses of $Zac1^{+/-}$ mice produced *Zac1*-homozygous null mice. To confirm the absence of normal Zac1 protein in adult homozygotes, we performed western blot analysis. In the wild-type pituitary gland, Zac1 antibody detected the two isoforms of the Zac1 protein arising from alternative splicing (Spengler et al., 1997), whereas neither isoform was detected in $Zac1^{-/-}$ homozygous pituitary glands (Figure 1C). Consistent with complete maternal silencing, no *Zac1* transcripts could be detected in E18.5 $Zac1^{+/-pat.}$ placenta and in several tissues from P1 $Zac1^{+/-pat.}$ heterozygous offspring (Figure 1D). Furthermore, immunohistochemistry of $Zac1^{+/-pat.}$ retinas demonstrated a complete loss of *Zac1* expression (data not shown) (L. Ma, N. Klenin, A.V., S. McFarlane, L.J., and C. Schuurmans, unpublished data). $Zac1^{+/-pat.}$ heterozygous offspring were then likely to behave phenotypically like homozygous offspring.

Intrauterine Growth Restriction in Mice Lacking *Zac1*

We compared the body weight at birth for all four possible genotypes. As expected for a maternally repressed gene, $Zac1^{+/-mat.}$ heterozygotes were indistinguishable from wild-type pups, whereas $Zac1^{+/-pat.}$ pups displayed a weight reduction that was also observed in $Zac1^{-/-}$ homozygotes (Figure 2A). Wild-type and homozygous $Zac1^{-/-}$ males were mated to wild-type females, and offspring was weighed at E13.5, E16.5, E18.5, and P0. Heterozygous $Zac1^{+/-pat.}$ mice displayed a highly significant reduction in body weight from E16.5 on (Figure 2B). The overall weight loss was 11% at E16.5 and 23% at birth, but was not similar for every organ. At E18.5, $Zac1^{+/-pat.}$ hind limb weight was reduced proportionally to the whole embryo body weight (Figure 2C), whereas the $Zac1^{+/-pat.}$ brain displayed no absolute weight change and was consequently larger relative to the embryo body weight. The reverse was observed for $Zac1^{+/-pat.}$ liver and lung whose weights were more strikingly reduced relative to the body weight of $Zac1^{+/-pat.}$ embryos (Figure 2C).

Because intrauterine growth restriction may result from impaired placental function, we assessed the functional status of wild-type and $Zac1^{+/-pat.}$ placentas. Loss of Zac1 function minimally affects placental weight

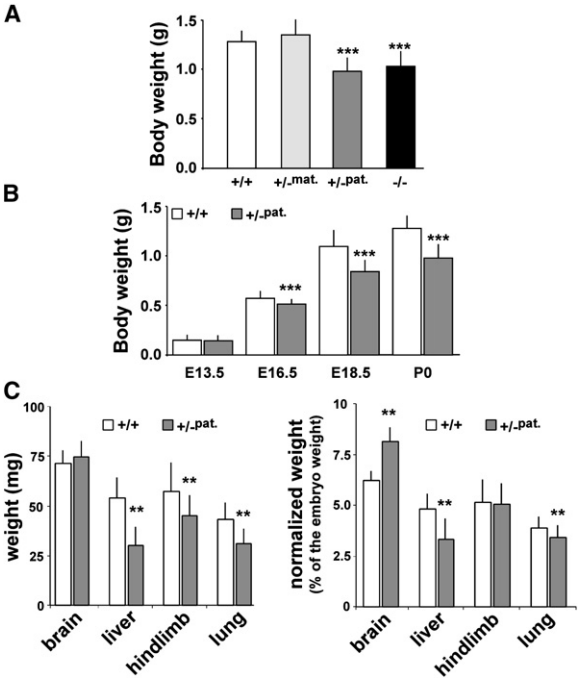

Figure 2. Intrauterine Growth Restriction in Mice Lacking *Zac1*

(A) Wild-type P0 pups (n = 188) were obtained by mating wild-type males and females. *Zac1*$^{+/-mat.}$ P0 pups (n = 25) were obtained by mating wild-type males to homozygous females. *Zac1*$^{+/-pat.}$ P0 pups (n = 231) were obtained by mating homozygous males to wild-type females. *Zac1*$^{-/-}$ P0 pups (n = 17) were obtained by mating homozygous males and females. The P0 pups were weighed immediately after birth, and the observed differences were tested using a Student's t test (triple asterisk, $p < 0.001$). Data are mean ± SD of the indicated number of animals.

(B) Wild-type or *Zac1*$^{-/-}$ males were mated to wild-type females to produce wild-type or *Zac1*$^{+/-pat.}$ embryos and pups. Offspring were weighed at E13.5 (+/+, n = 56; +/−pat., n = 31), E16.5 (+/+, n = 46; +/−pat., n = 43), E18.5 (+/+, n = 76; +/−pat., n = 69), and P0 (+/+, n = 96; +/−pat., n = 90). Data are mean ± SD of the indicated number of animals.

(C) E18.5 embryos were dissected, and organs were weighed: brain (+/+, n = 22; +/−pat., n = 24), liver (+/+, n = 59; +/−pat., n = 61), hindlimb (+/+, n = 54; +/−pat., n = 61), lung (+/+, n = 33; +/−pat., n = 34). Where indicated, the weight of the different organs was normalized to the weight of the corresponding embryo (double asterisk, $p < 0.01$). Data are mean ± SD of the indicated number of animals.

and does not significantly alter either placental histology or transport capacity of glucose and amino acids (see the Supplemental Results and Figure S1 in the Supplemental Data available with this article online).

Loss of *Zac1* Function Results in Altered Gross Morphology and Bone Formation

In addition to the consistently observed reduced weight, one third of *Zac1*$^{+/-pat.}$ pups displayed a severely altered gross morphology, including a curly tail and wrinkled skin (Figure 3A). Because *Zac1* is abundantly expressed in somites (Piras et al., 2000; Valente and Auladell, 2001) and chondrogenic tissues (Tsuda et al., 2004), we paid special attention to muscle and bone formation. We performed bone and cartilage staining on E18.5 embryos and evidenced altered ossification of the most caudal vertebrae, ankle bones (Figure 3B), and the last forelimb phalanx (Figure 3C).

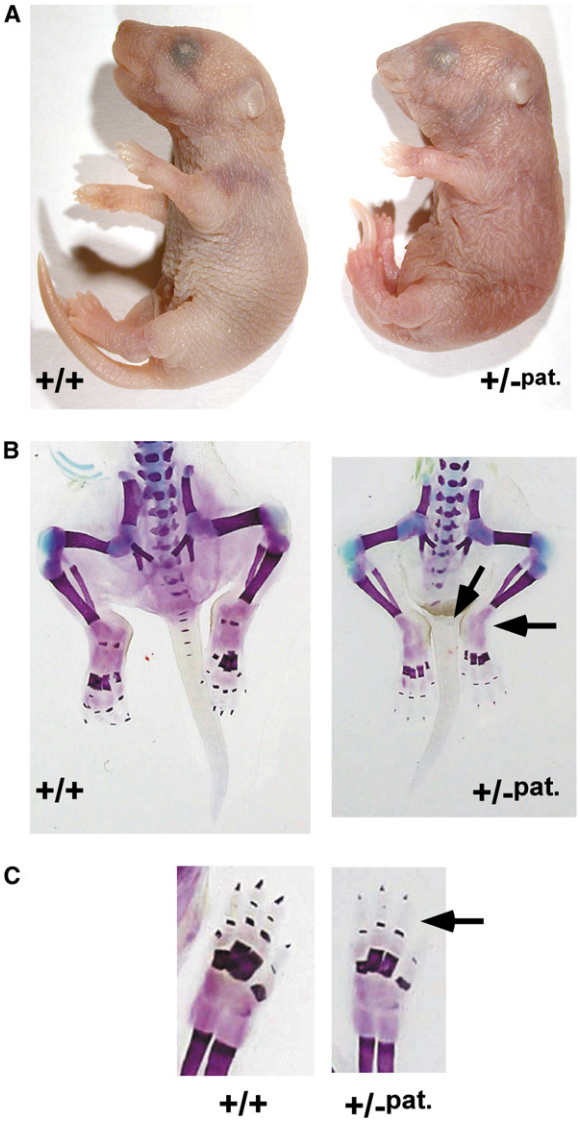

Figure 3. Lack of *Zac1* Alters Embryonic Development

(A) Wild-type and *Zac1*$^{+/-pat.}$ heterozygous pups were photographed at birth. The morphological defects of the *Zac1*$^{+/-pat.}$ pup, i.e., curled tail and wrinkled skin, were observed in one third of *Zac1*$^{+/-pat.}$ pups.

(B and C) Cartilage and bone of E18.5 wild-type and *Zac1*$^{+/-pat.}$ heterozygous embryos were stained with alcian blue and alizarin red. Consistent observations include ossification defects of the most caudal vertebrae, bones of the ankle, and last phalanx of the forelimb.

Impaired Postnatal Survival of *Zac1*$^{+/-pat.}$ Mice

Animals were routinely genotyped at 3 weeks postnatal, and we noticed that the transmission of the mutation was not Mendelian when of paternal origin. Mating of wild-type males to heterozygous females resulted in roughly equivalent numbers of wild-type and heterozygous pups (Figure 4A) (n = 302). In sharp contrast, mating of heterozygous males to wild-type females resulted in a drastically lower than expected number of heterozygous pups (Figure 4A) (n = 774). About 80% of the expected heterozygous pups were indeed missing. Mating of heterozygous males and females also resulted in

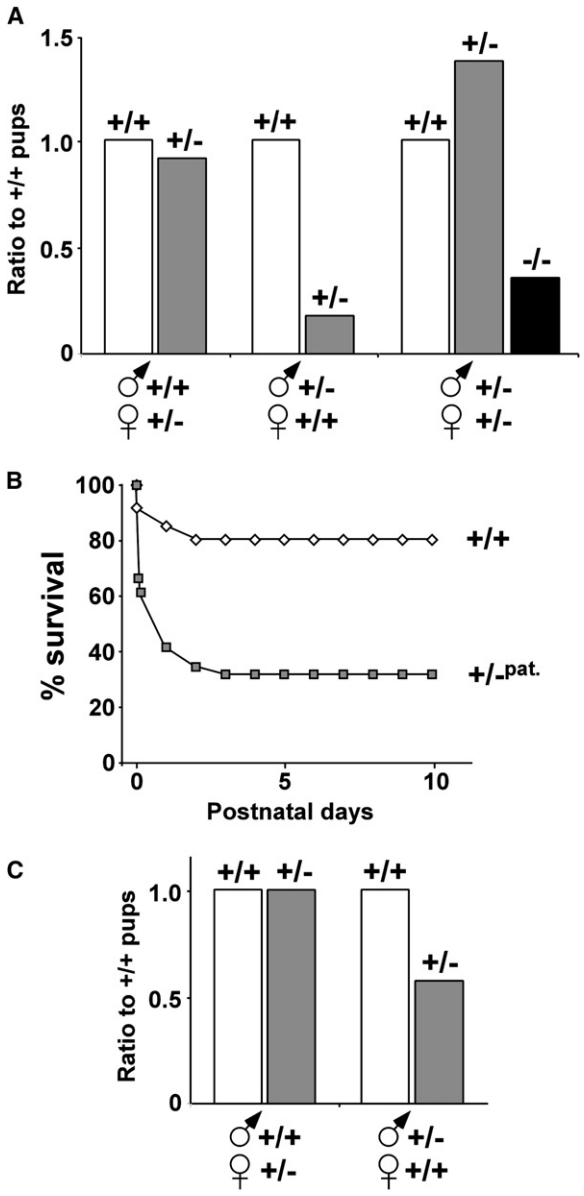

Figure 4. Loss of *Zac1* Function Impairs Postnatal Survival

(A) Wild-type C57BL/6 males were mated to C57BL/6 heterozygous females to produce wild-type and $Zac1^{+/-mat.}$ pups (n = 302). Heterozygous males were mated to wild-type females to produce wild-type and $Zac1^{+/-pat.}$ pups (n = 774). Heterozygous males and females were mated to produce all possible genotypes (n = 320). Pups were genotyped at 3 weeks postnatal, and the number of wild-type, heterozygous, and homozygous pups was expressed relative to the number of wild-type pups.

(B) $Zac1^{+/-pat.}$ pups die within 3 days post-natal. C57BL/6 wild-type and homozygous males were mated to C57BL/6 wild-type females to produce wild-type (n = 61) and $Zac1^{+/-pat.}$ heterozygous (n = 113) pups. Pups were monitored every 8 hr for the first 24 hr and then every day until weaning (P21).

(C) The same experiment as the one described in Figure 4A was performed with wild-type and heterozygous CBA mice. Wild-type CBA males were mated to heterozygous CBA females to produce wild-type and $Zac1^{+/-mat.}$ pups (n = 290). Heterozygous CBA males were mated to wild-type CBA females to produce wild-type and $Zac1^{+/-pat.}$ pups (n = 202).

reduced number of homozygous and heterozygous pups (Figure 4A) (n = 320).

We genotyped new born pups and embryos at different stages and found equal numbers of wild-type and heterozygous offspring from wild-type females mated to heterozygous males (data not shown). We concluded that the observed death occurred postnatally. We scrutinized newborn pups and noticed that many $Zac1^{+/-pat.}$ pups displayed dyspnea. Accordingly, about 50% died within 24 hr after birth, and an additional 20% died before postnatal day 3 (P3) (Figure 4B). We dissected and fixed lungs from a number of pups just after they died and observed that the lungs were either not or imperfectly inflated (data not shown). None of the pups with obvious malformation(s) survived more than 3 days. In addition, some morphologically normal pups also died. All pups that survived until P3 reached adulthood (Figure 4B).

Because all animals observed so far had a C57BL/6 genetic background, we asked whether the observed postnatal death was specific to this background. We performed similar experiments in a CBA background and also observed postnatal lethality of $Zac1^{+/-pat.}$ pups (Figure 4C). The extent of lethality was however reduced, suggesting that the effect of loss of *Zac1* function is modulated by genetic background.

Zac1 Belongs to a Network of Imprinted Genes that Regulate Embryonic Growth and Differentiation

To gain insights into *Zac1* mechanism of action, we searched for genes frequently coexpressed with *Zac1*. One of us (P.P.) recently reported a meta-analysis of a large set of human microarray data (Lee et al., 2004a). A similar study was performed on a body of 116 mouse microarray data sets, each data set containing 10 to >200 different samples. These data are freely accessible at http://microarray.genomecenter.columbia.edu/cgi-bin/find-links.cgi. We looked for genes coregulated with *Zac1/Plagl1* in this large set of microarray data and recorded the strength of each coexpression link (Lee et al., 2004a), i.e., the number of data sets in which *Zac1* was significantly coregulated with a given gene. We noticed that *Zac1* was frequently linked to other imprinted genes with a strength ≥ 2. Indeed, of 353 genes retrieved this way, 13 are imprinted, i.e., *Gtl2/AI852838* (strength = 7), *H19/X58196* (6), *Mest* (6), *Dlk1* (4), *Peg3* (4), *Grb10* (3), *Igf2* (3), *Igf2r* (3), *Dcn* (2), *Gnas* (2), *Gatm* (2), *Ndn* (2), *Slc38a4* (2). Since 34,018 mouse genes/ESTs, of which 60 are imprinted, were tested in at least two datasets, we computed a p value by using the binomial approximation to the hypergeometric distribution and worked out $p < 8 \times 10^{-15}$. We conclude that the clustering of *Zac1* with other imprinted genes in this type of analysis is highly significant. Accordingly, we hypothesized that *Zac1* might work together with other imprinted genes, prompting us to undertake a systematic search for genes linked to every imprinted gene with a strength ≥ 2. To focus on the genes most tightly linked to imprinted genes, we selected the 246 genes linked to at least three different imprinted genes with at least one link with a strength ≥ 4. To make the resulting network more accessible and easier to visualize, we only drew on Figure 5 the 442 links with a strength ≥ 4. The full list of genes and links is available as Supplemental Data. It

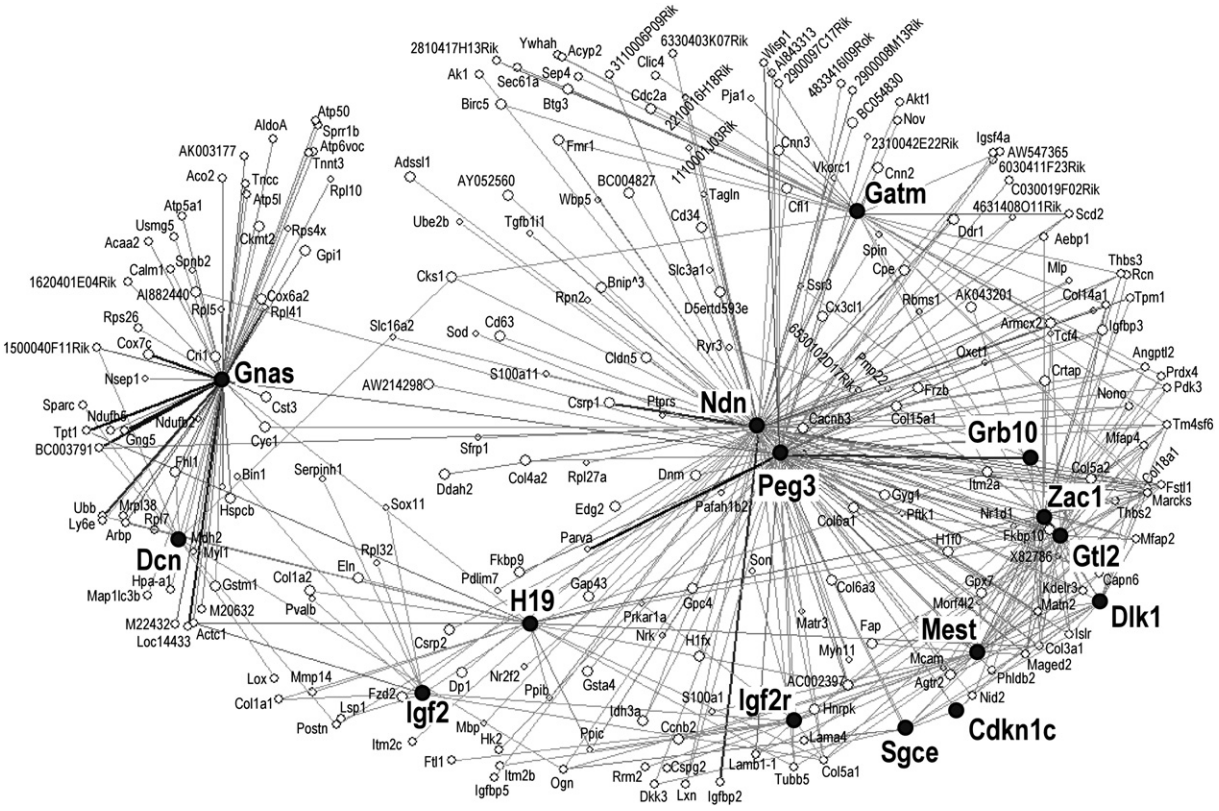

Figure 5. *Zac1* Belongs to a Network of Coregulated Imprinted Genes

Genes linked to imprinted genes, including *Zac1*, were searched for in a body of 116 microarray data sets, each comprising a minimum of ten samples. To facilitate the visualization of the resulting gene network, we selected the 246 genes linked to at least three imprinted genes and draw the 442 links with a strength ≥ 4 with Pajek software. The links between genes have different gray densities according to the number of data sets in which the genes are coregulated (light gray = 4 to black = 10).

should be emphasized that genes linked to only one imprinted gene on Figure 5 are in fact linked to at least two additional ones. For instance, although *Birc5* is apparently linked to only one imprinted gene (*Gatm*; strength = 4) on Figure 5, it is indeed connected to five additional ones (*Zac1*, *Peg3*, *Mest*, *Ndn*, *Gtl2*) with a strength < 4.

Zac1 Misexpression Alters the Expression of Several Imprinted Genes

To substantiate the affiliation of *Zac1* to the imprinted gene network (IGN) described above, we tested whether gain and loss of *Zac1* function alter the expression of genes comprised in this network. We focused on imprinted genes and designed and validated primers to perform real-time PCR for the 15 imprinted genes comprised in the IGN. Although *Slc38a4* is not represented on Figure 5 because it does not fulfill the criteria used to draw this network, it was included in the analysis because it is linked to *Zac1* as mentioned above and to other nonimprinted genes within the IGN (see the Supplemental Data). We used three primer pairs for the *Gnas* locus, i.e., *Gnas* exon1, *Gnas* exon1A, *Gnas* XL, because this complex locus includes three alternative promoters that give rise to transcripts encoding at least two different proteins (Plagge et al., 2004).

We first used a transient transfection paradigm and selected the Neuro2a neuroblastoma cell line, which is derived from postganglionic sympathetic neuroblasts that normally express *Zac1* during development (Piras et al., 2000), and lost *Zac1* expression upon transformation (Table 1). We achieved $\geq$95% transfection efficiency, and we verified that the level of *Zac1* expression following transfection is comparable to that measured in native tissues, e.g., embryonic and neonate brain, pituitary gland, tongue, hindlimb (data not shown). We compared the expression levels of imprinted genes 32 hr after transfection with cDNAs encoding chloramphenicol acetyl-transferase (CAT) as a control or *Zac1*. Using this strategy, we showed that *Zac1* re-expression in Neuro2a cells leads to the induction of several imprinted genes, notably *Igf2* (200×), *Cdkn1c* (16×), *H19* (11×), and *Dlk1* (1.8×) (Table 1). These changes in gene expression were unlikely to result from a proliferation shutdown or from the induction of apoptosis since they were also observed, with a lower magnitude, 10 hr following transfection, when neither growth arrest nor apoptosis is observed (data not shown).

We then tested whether changes in imprinted gene expression also occur following loss of *Zac1* function and performed a similar real-time PCR analysis of wild-type and $Zac1^{+/-pat.}$ E18.5 liver. We verified that the cell composition of mutant livers was not affected as this may complicate the interpretation of the observed regulations (Supplemental Results and Figure S2). Real-time PCR analysis revealed a statistically significant

Table 1. Gain and Loss of *Zac1* Function Elicit Opposite Regulation of *Cdkn1c*, *Igf2*, *H19*, and *Dlk1*

	Neuro2a						Liver					
Gene Name	CAT	SD	Zac1	SD	Zac1/CAT	p<	+/+	SD	+/−pat.	SD	+/−pat./+/+	p<
Cdkn1c/Kip2	0.012	0.004	0.191	0.013	**16.13**	**0.001**	11.977	1.856	6.471	1.226	**0.54**	**0.001**
Dcn	*0.003*	*0.002*	*0.008*	*0.001*	—		1.389	0.097	1.689	0.096	**1.22**	**0.001**
Dlk1/Pref1	0.640	0.027	1.139	0.032	**1.78**	**0.001**	6.767	0.395	5.195	0.488	**0.77**	**0.001**
Gatm	*0.000*	*0.000*	*0.000*	*0.000*	—		0.390	0.016	0.369	0.028	0.95	NS
Gnas exon1	10.03	1.933	14.514	2.333	1.45	NS	0.522	0.057	0.596	0.107	1.14	NS
Gnas exon1A	0.143	0.047	0.252	0.045	1.77	NS	0.004	0.002	0.006	0.002	1.36	NS
Gnas XL	0.657	0.102	1.606	0.565	2.45	NS	0.041	0.008	0.059	0.008	**1.42**	**0.010**
Grb10	*0.003*	*0.002*	*0.000*	*0.000*	—		12.694	0.749	9.845	0.911	**0.78**	**0.001**
Gtl2	0.020	0.003	0.080	0.010	**4.11**	**0.001**	5.764	0.173	5.199	0.519	0.90	NS
H19	0.005	0.001	0.056	0.006	**10.92**	**0.001**	515.011	57.420	424.644	24.831	**0.82**	**0.010**
Igf2	0.002	0.001	0.368	0.034	**199.58**	**0.001**	98.463	11.412	72.216	7.149	**0.73**	**0.001**
Igf2r	*0.001*	*0.001*	*0.003*	*0.001*	—		0.749	0.081	0.661	0.059	0.88	NS
Mest	12.80	2.009	19.398	0.461	**1.52**	**0.010**	2.937	0.204	3.459	0.215	**1.18**	**0.010**
Ndn	*0.000*	*0.000*	*0.000*	*0.000*	—		0.096	0.004	0.093	0.018	0.97	NS
Peg3	1.270	0.178	1.550	0.145	1.22	NS	1.531	0.116	1.529	0.092	1.00	NS
Sgce	0.658	0.111	0.670	0.029	1.02	NS	0.486	0.066	0.481	0.034	0.99	NS
Slc38a4	*0.001*	*0.001*	*0.002*	*0.001*	—		2.658	0.124	2.538	0.179	0.95	NS
Zac1	*0.000*	*0.001*	*0.001*	*0.000*	—		1.511	0.034	0.000	0.000	—	

Neuro2a cells were transiently transfected with chloramphenicol acetyltransferase (CAT) or *Zac1*. Total RNA from three independent transfections was used to generate cDNAs in three independent reverse-transcription reactions. Liver was dissected from E18.5 wild-type (+/+) and *Zac1*-deficient (+/−pat.) embryos. Total RNA from 12 embryos of each genotype from two independent litters was pooled and reverse transcribed in three independent reactions to produce cDNAs. Imprinted gene expression levels were determined in duplicate in each cDNA preparation by real-time PCR. Expression levels of each imprinted gene was normalized to that of three housekeeping genes. Average of normalized expression levels (CAT; Zac1; +/+; +/−pat.), standard deviation (SD), ratio (Zac1/CAT; +/−pat. / +/+), and p value (Student's t test) are displayed for each imprinted gene. Primers used to quantify *Zac1* in Neuro2a cells are located in the 3′UTR and do not detect the transfected *Zac1* cDNA. Primers to quantify *Zac1* expression in E18.5 liver are located in the coding region that was deleted by homologous recombination. Ratios and p values in bold denote significantly differentially expressed genes. Values in italics correspond to genes called absent. NS, not significant.

downregulation of the imprinted genes that were found upregulated in *Zac1*-transfected Neuro2a cells, i.e., *Igf2* (1.4×), *Cdkn1c* (1.9×), *H19* (1.2×), and *Dlk1* (1.3×) (Table 1).

Zac1 Binds to *H19* 3′ Enhancers, which Results in Transactivation of *Igf2* and *H19* Promoters

Given the phenotype of the *Igf2*-, *H19*-, *Cdkn1c*-, and *Dlk1*-deficient mice, the downregulation of these genes in *Zac1*-deficient liver possibly accounts for the growth restriction phenotype of *Zac1*-deficient mice. We hence tested whether Zac1 is a direct regulator of these genes. We focused on *Igf2* and *H19* because the genes are adjacent on mouse chromosome 7 but are expressed from the paternal and maternal chromosome, respectively. Zac1 could then independently regulate each gene through binding to their respective promoters; alternatively, Zac1 could bind to a shared regulatory element. We noticed that the *H19* locus comprises several Zac1 consensus binding sites (G_4C_4) (Figure 6A) (Hoffmann et al., 2003; Varrault et al., 1998), notably in each of the two endodermal enhancers located 3′ of *H19* (Leighton et al., 1995). We performed chromatin immunoprecipitation on *Zac1*-transfected Neuro2a and MIN6 cells (Figure 6B). For Neuro2a cells, three independent chromatin preparations were made, immunoprecipitated in duplicate, and quantified in duplicate. For MIN6 cells, nine independent chromatin preparations were made, immunoprecipitated, and quantified in duplicate. To assess for the statistical significance of the observed differences, we performed a one-sided, paired permutation test with exact statistics. No Zac1 binding was observed in the *Igf2* gene (data not shown). We showed significant binding of Zac1 to the *H19* enhancer region in both cell lines and a weaker binding to the *H19* promoter in MIN6 cells (Figure 6B).

To test for the functional correlate of Zac1 binding, we constructed plasmids containing the Luciferase cDNA as a reporter gene (Figures 6C and 6D). Luciferase was flanked on the 5′ side by either a minimal TATA box derived from the adenoviral E1B promoter, the *H19* promoter, or the P3 *Igf2* promoter. It was flanked downstream of the polyadenylation site by either no specific sequence or the *H19* enhancers, alone or in combination. We transfected these constructs together with cDNAs encoding chloramphenicol acetyl-transferase (CAT) as a control or *Zac1* in HepG2 hepatocarcinoma cells, in which the *H19* enhancers were previously shown to work in reporter assays (Long and Spear, 2004; Yoo-Warren et al., 1988). Eight independent transfections with two different plasmid preparations were carried out. To assess for statistical significance of the observed differences, we performed a two-sided, paired permutation test with exact statistics. As expected, the enhancers were active on the *H19* (Figure 6C) and *Igf2* P3 (Figure 6D) promoters but not on the minimal E1B TATA box (data not shown). Remarkably, Zac1 potentiated the effect of the E2 enhancer on both promoters (Figures 6C and 6D). Because we detected a weak Zac1 binding to the *H19* promoter in MIN6 cells, we also tested for transactivation of this promoter in these cells. We observed a significant 2.1-fold stimulation of the luciferase activity following *Zac1* transfection (data not shown). The effect of Zac1 on *H19* enhancers could, however, not be tested in this cell line because the enhancers showed no effect per se on either the *H19* or

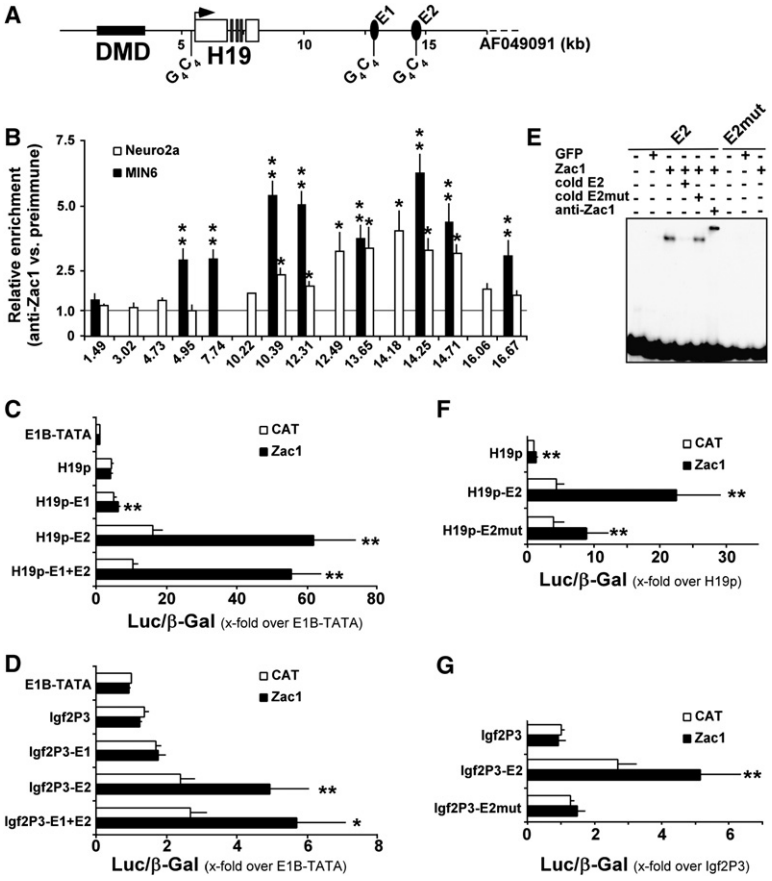

Figure 6. Zac1 Binds to the Endodermal Enhancers Downstream of *H19* and Transactivates *H19* and *Igf2* Promoters

(A) Simplified map of the *H19* locus. DMD denotes the intergenic differentially methylated region between *Igf2* and *H19*. G_4C_4 denotes Zac1 consensus binding sites (Hoffmann et al., 2003; Varrault et al., 1998). Closed ovals indicate the location of endodermal enhancers.

(B) Real-time PCR scan of the *H19* locus following chromatin immunoprecipitation. MIN6 and Neuro2a cells were transfected with a plasmid encoding Zac1. Chromatin immunoprecipitation with anti-Zac1 and preimmune sera was performed as described in the Experimental Procedures. The amount of immunoprecipitated material was quantified by real-time PCR with primers located throughout the *H19* locus. The relative enrichment fold (anti-Zac1/preimmune) is plotted against the position of the primer pair used for real-time PCR on contig AF049091. Data are mean ± SEM of six (Neuro2a) or nine (MIN6) independent immunoprecipitations. p values were computed with exact statistics in a one-sided, paired permutation test (asterisk, $p < 0.05$; double asterisk, $p < 0.01$).

(C) Zac1 binding to the E2 enhancer regulates the activity of the *H19* promoter. A minimal TATA box from the adenovirus E1B promoter or a PCR fragment comprising 440 bp from the *H19* promoter was subcloned upstream of the Luciferase cDNA. PCR fragments containing the *H19* E1 and E2 enhancers were subcloned downstream of the SV40 polyadenylation site. The reporter plasmids were transfected into hepatocarcinoma HepG2 cells together with plasmids encoding CAT or Zac1. Data are mean ± SEM of eight independent transfections quantified in triplicate. p values were computed with exact statistics in a two-sided, paired permutation test (asterisk, $p < 0.05$; double asterisk, $p < 0.01$).

(D) Zac1 binding to the E2 enhancer regulates the activity of the *Igf2* P3 promoter. Same as in (C) with a 760 bp fragment from the *Igf2* P3 promoter.

(E) Zac1 binds to the *H19* 3′ E2 enhancer, and mutation of the G_4C_4 Zac1 consensus binding site abolishes Zac1 binding. Electrophoretic mobility shift assay (EMSA) was performed with nuclear extracts from GFP- and Zac1-transfected Neuro2a cells as described in the Experimental Procedures. The specificity of the binding is demonstrated by competition with a 10-fold excess of the cold probe (cold E2) or of the cold mutated probe (cold E2mut) and incubation with the anti-Zac1 antibody resulting in supershift of the E2 probe.

(F) Same as in (C) with a wild-type or a mutated Zac1 binding site in the E2 enhancer. Data are mean ± SD of four independent transfections quantified in triplicate. p values were computed with exact statistics in a two-sided, paired permutation test (double asterisk, $p < 0.01$).

(G) Same as in (F) with a 760 bp fragment from the *Igf2* P3 promoter.

the *Igf2* P3 promoter, as previously reported in other cell lines (Yoo-Warren et al., 1988).

Zac1 Potentiates E2 Activity through Binding to Its Consensus Binding Site

To further characterize the regulation of the E2 enhancer activity by Zac1, we assessed the direct binding of Zac1 to E2. We performed EMSA with an oligonucleotide located in the E2 region and comprising the Zac1 consensus binding site (G_4C_4). We showed that nuclear extracts from Zac1-transfected Neuro2a cells shift the oligo, whereas those prepared from GFP-transfected cells do not (Figure 6E). Furthermore, mutation of the G_4C_4 sequence to G_3ATC_3 abolished Zac1 binding (Figure 6E). The specificity of Zac1 binding was further demonstrated by competition with a 10-fold excess of cold wild-type or mutated E2 probes and by supershifting with the anti-Zac1 antibody. We introduced a similar mutation in the plasmids used in Figures 6C and 6D and verified that abolition of Zac1 binding to its consensus site in the E2 region alters its functional activity (Figures 6F and 6G). The potentiation by Zac1 of E2 activity toward the H19 promoter was drastically reduced (Figure 6F), indicating that Zac1 binding to its consensus binding site within E2 is required for its full activity and that Zac1 also works through another interaction with E2. This interaction could be direct through binding to a cryptic site in E2; it could also be indirect since Zac1 was shown to work as a coactivator of other transcription factors such as nuclear receptors (Huang and Stallcup, 2000) and p53 (Huang et al., 2001; Rozenfeld-Granot et al., 2002). The effect of the mutation on the *Igf2*-P3 promoter was even more drastic as Zac1 was not able to potentiate the effect of mutated E2 toward this promoter (Figure 6G). Indeed, mutation of Zac1 consensus binding site within E2 fully abolished its enhancer activity (Figure 6G), suggesting that this sequence is absolutely required for E2 activity toward *Igf2*-P3. Altogether, these data indicate that Zac1 robustly binds to the *H19* 3′ E2 enhancer, which results in transactivation of the *H19* and *Igf2* promoters.

Discussion

The present report demonstrates that *Zac1* belongs to the class of imprinted genes involved in embryonic growth control since loss of *Zac1* function resulted in intrauterine growth restriction. This observation was made in offspring from wild-type females mated to homozygous males, which implies that growth restriction does not result from a shortcoming of the mother or from competition between embryos of different genotypes. It is therefore concluded that the growth defect is intrinsic to the conceptus. Intrauterine growth restriction potentially results from an intrinsically defective growth of the embryo and/or an impaired transport of nutrients across the placenta (Reik et al., 2003). Although *Zac1* is expressed in the placenta, the placental function was not affected in *Zac1* mutant mice (Supplemental Data), which is in favor of a direct effect of *Zac1* on embryonic growth.

The embryonic growth restriction phenotype observed in *Zac1*-deficient mice is counterintuitive. Indeed, it is generally observed that inactivation of genes promoting cell proliferation, e.g., oncogenes, leads to growth restriction, and inactivation of genes restraining cell proliferation, e.g., tumor suppressor genes, leads to overgrowth (Ciemerych and Sicinski, 2005). For instance, the inactivation of *Igf2* induces intrauterine growth restriction (DeChiara et al., 1990), and the inactivation of *Igf2r* (Wang et al., 1994) results in embryonic overgrowth. It was therefore unexpected that the inactivation of *Zac1*, a putative tumor suppressor gene with proapoptotic and cell-cycle-blocking activities, results in embryonic growth restriction. On the other hand, the kinship theory predicts that paternally expressed imprinted genes are growth promoting, and maternally expressed genes are growth restraining. The growth restriction phenotype of *Zac1*-deficient embryos shows that *Zac1* complies with the kinship theory and accounts for the paternal expression of this antiproliferative gene. Therefore, evolution selected a limited number of genes to be imprinted according to their physiological properties rather than their molecular functions.

To gain insights into *Zac1* mechanism of action, we used the results of a meta-analysis of 116 microarray data sets and searched for genes frequently coregulated with *Zac1*. The underlying assumption is that genes that cluster together would share biological function (Fraser and Marcotte, 2004). This approach proved extremely informative in relatively simple model organisms such as yeast (Lee et al., 2004b; Wu et al., 2002) and *C. elegans* (Kim et al., 2001) but is still not widely used for mammals (Lee et al., 2004a; Zhang et al., 2004). We noticed that the set of genes most closely linked to *Zac1* displayed a statistically highly significant overrepresentation of imprinted genes, i.e., *Gtl2*, *H19*, *Mest*, *Dlk1*, *Peg3*, *Grb10*, *Igf2*, *Igf2r*, *Dcn*, *Gnas*, *Gatm*, *Ndn*, *Slc38a4*. We made a more systematic search for genes linked to imprinted genes and focused on the network of imprinted and nonimprinted genes that were the most densely connected. Because of the phenotype of *Zac1* null mice, and because mutants of numerous other imprinted genes in this network also display alterations in embryonic development, we conclude that *Zac1* is a member of an imprinted genes network (IGN) that controls embryonic growth and differentiation. This observation is certainly of interest to understand *Zac1* biology. It is also relevant in the context of imprinting in general. Indeed, the IGN we describe in this report may well be the network of genes involved in the control of embryonic growth that was supposedly targeted by imprinting during mammalian evolution (Reik and Lewis, 2005). Additional experiments will be necessary to test whether a similar network of coregulated genes existed before the emergence of imprinting during mammalian evolution.

A general feature of gene networks is to adapt to genetic and environmental changes by altering the expression of genes they consist of. This is the origin of robustness against mutations during development (Siegal and Bergman, 2002; Wagner, 2000) and frequently underlies epistasis (Moore, 2005; Segre et al., 2005). To confirm that *Zac1* belongs to the IGN, we tested whether this network is transcriptionally perturbed by *Zac1* misexpression. We first analyzed transiently transfected cells because this experimental setting provides an opportunity to look at the acute transcriptional response to Zac1. We observed a large induction of *Igf2*, *Cdkn1c*, and *H19* and a moderate but statistically significant induction of *Gtl2*, *Dlk1*, and *Mest*. We then performed a similar analysis of E18.5 wild-type and *Zac1*-deficient liver. In this setting, the gene network is given time to adapt to loss of *Zac1* function and is supposed to reach a novel stable state compatible with an almost normal embryonic development. We observed a significant downregulation of some of the genes, i.e., *Cdkn1c*, *Igf2*, *H19*, and *Dlk1*, which were vigorously induced by *Zac1* re-expression in Neuro2a cells. Another strong argument in favor of the existence of the IGN, and *Zac1*'s affiliation to it, is the demonstration of a direct functional link between *Zac1* and other imprinted genes. Arima and coworkers recently suggested that human ZAC regulates the expression of *CDKN1C* through binding to the CpG island and upregulation of *LIT1/KCNQ1OT1*, an antisense imprinted gene thought to negatively regulate *CDKN1C* (Arima et al., 2005). Though we could not confirm the regulation of mouse *Lit1* by *Zac1* in real-time PCR experiments (data not shown), we observed that deregulated *Zac1* expression does alter *Cdkn1c* expression. In the present report, we focused on *Igf2* and *H19* because they are adjacent on mouse chromosome 7 and are reciprocally imprinted. We showed that Zac1 binds to and regulates the activity of the E2 enhancer located downstream of *H19* and shared with *Igf2*. Zac1, as well as FoxA that was recently showed to bind the E1 enhancer (Long and Spear, 2004), therefore participates into the regulation of the *Igf2*/*H19* locus. Zac1 could be involved in the remodeling of the complex architecture of this locus (Murrell et al., 2004) and/or could work as a transcriptional activator or coactivator once the appropriate chromatin loops are formed since both activities were associated with Zac1 (Hoffmann et al., 2003; Huang and Stallcup, 2000). Whatever the mechanistic details are, we showed that *Zac1* is upstream of *Igf2*/*H19*, *Cdkn1c*, and *Dlk1* in a genetic network aimed at controlling embryonic growth.

Deregulation of these genes in *Zac1*-deficient mice is likely to account for the observed growth-restriction phenotype. Indeed, *Igf2* (DeChiara et al.,

1990), *Cdkn1c/Kip2* (Takahashi et al., 2000), and *Dlk1/Pref1* (Moon et al., 2002) knockout mice display growth restriction. The extent of *Igf2* deregulation in *Zac1*-deficient liver is limited (~25%–30%), but it should be emphasized that complete loss of *Igf2* expression in knockout mice resulted in 40% reduction of body weight at birth (DeChiara et al., 1990), while *Zac1* deficiency results in 23% body weight reduction. Furthermore, the concomitant downregulation of several growth-promoting imprinted genes within the IGN, i.e., *Igf2*, *Cdkn1c*, and *Dlk1*, is likely to have additive effects and to result in major defect of the biological function conveyed by this network. It is also noteworthy that the growth-restraining imprinted gene *Grb10* is downregulated in *Zac1*-deficient liver. *Grb10* inactivation results in embryonic overgrowth, which is partially compensated by *Igf2* inactivation (Charalambous et al., 2003). The observed *Grb10* downregulation in *Zac1*-deficient mice likely corresponds to a homeostatic regulation of the IGN aimed at antagonizing *Zac1* deficiency and *Igf2*, *Cdkn1c*, and *Dlk1* downregulation. This observation further illustrates the mechanisms at work to safeguard the robustness of gene networks and of their associated biological function(s). Collectively, our data show that *Zac1* is a bona fide member of the IGN and suggest that *Zac1* deficiency affects embryonic growth through the deregulation of other imprinted genes, namely *Igf2*, *Cdkn1c*, and *Dlk1*.

Imprinted genes within the IGN have a pattern of connectivity that is reminiscent of scale-free networks (Barabasi and Albert, 1999). *Peg3*, *Ndn*, *Gnas*, and *Gatm* correspond to hub-like nodes, i.e., they are connected to a large number of genes. On the other hand, *Igf2*, *Igf2r*, *H19*, *Sgce*, *Cdkn1c*, *Grb10*, *Zac1*, *Gtl2*, *Dlk1*, and *Mest* have a lower degree of connectivity. Additional work will be necessary to determine if the latter class of imprinted genes represents the input and regulatory core of the network, while genes of the hub-like class ensure the connection to effector genes. The meta-analysis of microarray data also raises new hypotheses with respect to the biochemical processes controlled by *Zac1* and by other imprinted genes. It is worth mentioning that genes that encode extracellular matrix (ECM) proteins are overrepresented in the IGN. Because the data sets in which imprinted genes were most frequently coexpressed correspond to regenerating and developing muscle (data not shown), an attractive hypothesis is that the biological function associated with the IGN is the control of cell adhesion-related processes during embryonic muscle development.

A recent study suggests that the IGN may also constitute a key safeguard against neoplasm formation in adults. Holm and coworkers (Holm et al., 2005) showed that global loss of imprinting (LOI), resulting from targeted inactivation of *Dnmt1* in ES cells, most notably affects expression of *Zac1* (2.2×), *Peg3* (1.8×), *Sgce* (1.6×), *Ndn* (1.6×), *Igf2r* (0.4×), *Cdkn1c* (0.3×), and *Grb10* (0.1×), which all belong to the IGN. Interestingly, among the very few nonimprinted genes differentially expressed in imprint-free versus control MEFs are found several genes that belong to the IGN, i.e., *Matn2*, *Itm2a*, *6330403K07Rik*, *Col18a1*, and *Dnmt3a*. The result of the global LOI was the immortalization of embryonic fibroblasts and the formation of hepatocellular carcinomas and intestinal adenomas. In this study, the methylation status of the *Igf2/H19* locus was variably affected, but other studies previously demonstrated the importance of *Igf2* LOI in tumor formation (Ohlsson, 2004). Altogether, these data indicate that, in addition to its effect during embryonic development, alteration of the biochemical process(es) controlled by the IGN is sufficient to initiate tumor formation and sustain tumor development in adults.

Experimental Procedures

Generation and Genotyping of *Zac1*-Deficient Mice

Two overlapping clones, C26 and C35 comprising the two last exons of mouse *Zac1*, were obtained by screening a 129/Sv genomic library (a generous gift by Dr. Philippe Soriano, FHCRC, Seattle) constructed in λDashII (Stratagene). The targeting vector was made by successive subcloning into pBSII-SK(-) of (1) a 2.5 kb *Not* I/*Pst* I fragment from clone C35, corresponding to a portion of the intron 5′ of the first coding exon of *Zac1* and a small portion of the λDashII vector, (2) a *Xho* I/*Hind* III fragment containing the pPolII promoter and the Neo resistance gene, (3) a 5.5 kb *Ava* I fragment from clone C26 corresponding to most of the last exon of *Zac1* and a small portion of the λDashII vector, and (4) a *Sal* I fragment containing the thymidine kinase cassette. The targeting vector (50 μg) was linearized with *Not* I and electroporated into 9×10^6 H1 ES cells (a gift by Drs. A. Dierich and P. Chambon, IGBMC, Strasbourg). ES cells were plated onto mitomycin C-treated fibroblasts and selected with G418 (180 μg/ml) and gancyclovir (2 μM) for 2 weeks. One hundred and sixty-one double resistant clones were expanded and screened by Southern blotting of *Kpn*I-digested genomic DNA with appropriate PCR fragments as 5′ and 3′ probes. Homologous recombination resulted in a size shift from 8.0 to 12.8 kb. Five positive clones were confirmed by PCR with primers KOZ-i1, KOZ-5nc, and KOZ-pPOL (Table S1). Cells from five positive clones were injected into C57BL/6 blastocysts and implanted into pseudopregnant females. Chimeric offspring were bred to C57BL/6 mice (Charles River France) to produce $Zac1^{+/-}$ offspring that were bred to C57BL/6 mice for nine additional generations. Genotyping was routinely performed with Taqman probes and primers specific for the wild-type (Zac-2406T; Zac-2382F; Zac-2449R) and knockout (KOpA-1605T; KopA-1582F; KopA-1643R) alleles (Table S1).

Skeletal Staining

E18.5 embryos were skinned, eviscerated, and fixed overnight in 100% ethanol. They were stained with alcian blue and alizarin red as previously described (Vivian et al., 2000).

Construction of the Gene Network

Data from 116 mouse microarray experiments containing a minimum of ten biological samples per experiment were analyzed exactly as in Lee et al. (2004a). The description of all data sets used in the meta-analysis is publicly available at http://microarray.genomecenter.columbia.edu/cgi-bin/datasetInfo.cgi. The genes linked to each imprinted gene with a strength ≥ 2, i.e., in at least two independent experiments, were retrieved. Only those 246 genes linked to at least three different imprinted genes were considered for the analysis. The resulting network was visualized with Pajek software (http://vlado.fmf.uni-lj.si/pub/networks/pajek/). To make the network easier to visualize, we only drew on Figure 5 the 442 links with a strength ≥ 4.

Plasmids, Cell Culture, and Transfection

Plasmids encoding β-galactosidase, chloramphenicol acetyl-transferase (CAT), and Zac1 were described previously (Spengler et al., 1997). Neuro2a, a mouse neuroblastoma-derived cell line, HepG2, a human hepatocarcinoma cell line, and MIN6, a mouse β-pancreatic cell line, were routinely cultured in DMEM supplemented with fetal bovine serum and penicillin-streptomycin (Invitrogen). Cells were transfected with Lipofectamine 2000 (Invitrogen) according to the manufacturer's instructions.

Analysis of the Expression Level of Imprinted Genes

Total RNA was harvested from Neuro2a cells 32 hr after transfection and from E18.5 wild-type and *Zac1*$^{+/-pat.}$ liver. We extracted total RNA from tissues or cells with Trizol reagent (Invitrogen) according to the manufacturer's instructions. We carried out RT-PCR analysis of total RNA with random hexamer oligonucleotides for reverse transcription. The sequences of the primers used for the determination of imprinted gene expression levels are given in Table S2. The selection of appropriate housekeeping genes was performed with geNorm (Vandesompele et al., 2002). The level of expression of each imprinted gene X was normalized to the geometric mean of the expression levels of three housekeeping genes (*Hprt*, *Tbp2*, and *Tubb2* for Neuro2a cells; *B2m*, *Gus*, and *Trfr* for E18.5 liver), according to the formula: X/geometric mean (R1, R2, R3) = $2^{(Ct[X]-\text{arithmetic mean } [Ct(R1),Ct(R2),Ct(R3)])}$, where Ct is the threshold cycle, and R1, R2, R3 are the three reference genes.

Chromatin Immunoprecipitation

ChIP was performed by a standard protocol (Kouskouti et al., 2004). Briefly, MIN6 or Neuro2a cells were fixed in culture medium with 1% formaldehyde for 10 min at 37°C. The cells were then washed in PBS and lysed in hypotonic buffer. The nuclei were resuspended in a buffer containing 0.1% SDS. The chromatin was fragmented for 20 min at 4°C with a Bioruptor sonicator (Diagerode, Liège, Belgium). Average length of sonicated fragments was 0.3–0.5 kb for Neuro2A cells and 0.5–1 kb for MIN6 cells. Diluted chromatin was incubated overnight with a rabbit preimmune serum or a serum raised against a GST-Zac1 fusion protein (Spengler et al., 1997). The chromatin was then collected with protein A-Sepharose beads and extensively washed. Each immunoprecipitate was assessed by real-time PCR with primers located in the *Igf2/H19* locus or in three control loci (*Blvrb*, *5H24*, *Vgcnl*) for normalization. Real-time PCR data were normalized for each immunoprecipitate to the geometric mean of the PCR signals obtained in the same immunoprecipitate with primers located in the three unrelated control loci. The sequences of the primers used for real-time PCR are given in Table S3.

Enhancer Assay

The *H19* endodermal enhancers E1 and E2 were PCR amplified with appropriate primers (Table S4), alone or in combination, and cloned downstream of the Luciferase/SV40 polydenylation cassette in pGL2 (Promega). A minimal TATA box from the E1B promoter (Hoffmann et al., 2003), a PCR fragment comprising 440 bp from the *H19* promoter (see Table S4 for the primer sequences), or a NheI/SacI fragment containing 760 bp from the *Igf2* P3 promoter derived from pP3L (Caricasole and Ward, 1993) were subsequently cloned upstream of the Luciferase cDNA. The G_4C_4 sequence of the E2 enhancer (14,452–14,459 in AF049091) was mutated to G_2ATATC_2 with QuikChange II XL site-directed mutagenesis kit (Stratagene). Mutated plasmids were identified by the newly created EcoR V restriction site. Sequences were verified by sequencing both strands. Plasmids were transfected into HepG2 hepatoma cells, and Luciferase and β-galactosidase activity were measured 24 hr later as previously described (Varrault et al., 2001).

Electrophoretic Mobility Shift Assay

EMSA was performed as previously described (Bilanges et al., 2001). Briefly, 25-mer oligonucleotides (Table S6) comprising the Zac1 consensus-binding site (G_4C_4) or a mutated sequence (G_3ATC_3) were annealled and labeled with T4 polynucleotide kinase and ^{32}P-γATP. They were incubated with no nuclear extract or nuclear extracts from GFP- or Zac1-transfected Neuro2a cells. The specificity of the binding is demonstrated by competition with a 10-fold excess of the cold probe (cold E2) or of the cold mutated probe (cold E2mut) and incubation with the anti-Zac1 antibody. DNA-protein complexes were separated from free probe on a 7% polyacrylamide gel.

Supplemental Data

Supplemental Data include a detailed analysis of the functional status of Zac1-deficient placenta (Figure S1), an histological and microarray characterization of Zac1-deficient liver (Figure S2 and Supplemental Results), and a list of primers used in this study (Tables S1–S6) and are available at http://www.developmentalcell.com/cgi/content/full/11/5/711/DC1/.

Acknowledgments

We are grateful to Drs. P. Arnaud, R. Feil, T. Forne, and C. Schuurmans for critical reading of the manuscript; to Dr. P. Jay for helping with histological procedures; to Drs. N. Negre and G. Cavalli for helping with the ChIP experiments; to Dr. M.J. Villarem for the gift of HepG2 cells; and to Dr. A. Plagge for helping with the Gnas locus. C.G. is a recipient of a fellowship from the Ministère de l'Education et de la Recherche. This work was supported by grants from the Centre National de la Recherche Scientifique, the Fondation Schlumberger pour l'Education et la Recherche, the Association pour la Recherche contre le Cancer, and the European Community (CT-1999-00602) to L.J. The authors declare that they have no competing financial interests.

Received: July 11, 2005
Revised: June 13, 2006
Accepted: September 5, 2006
Published: November 6, 2006

References

Arima, T., Kamikihara, T., Hayashida, T., Kato, K., Inoue, T., Shirayoshi, Y., Oshimura, M., Soejima, H., Mukai, T., and Wake, N. (2005). ZAC, LIT1 (KCNQ1OT1) and p57KIP2 (CDKN1C) are in an imprinted gene network that may play a role in Beckwith-Wiedemann syndrome. Nucleic Acids Res. *33*, 2650–2660.

Barabasi, A.L., and Albert, R. (1999). Emergence of scaling in random networks. Science *286*, 509–512.

Basyuk, E., Coulon, V., Le Digarcher, A., Coisy-Quivy, M., Moles, J.P., Gandarillas, A., and Journot, L. (2005). The candidate tumor suppressor gene ZAC is involved in keratinocyte differentiation and its expression is lost in basal cell carcinomas. Mol. Cancer Res. *3*, 483–492.

Bilanges, B., Varrault, A., Basyuk, E., Rodriguez, C., Mazumdar, A., Pantaloni, C., Bockaert, J., Theillet, C., Spengler, D., and Journot, L. (1999). Loss of expression of the candidate tumor suppressor gene ZAC in breast cancer cell lines and primary tumors. Oncogene *18*, 3979–3988.

Bilanges, B., Varrault, A., Mazumdar, A., Pantaloni, C., Hoffmann, A., Bockaert, J., Spengler, D., and Journot, L. (2001). Alternative splicing of the imprinted candidate tumor suppressor gene ZAC regulates its antiproliferative and DNA binding activities. Oncogene *20*, 1246–1253.

Caricasole, A., and Ward, A. (1993). Transactivation of mouse insulin-like growth factor II (IGF-II) gene promoters by the AP-1 complex. Nucleic Acids Res. *21*, 1873–1879.

Cattanach, B.M., and Kirk, M. (1985). Differential activity of maternally and paternally derived chromosome regions in mice. Nature *315*, 496–498.

Charalambous, M., Smith, F.M., Bennett, W.R., Crew, T.E., Mackenzie, F., and Ward, A. (2003). Disruption of the imprinted Grb10 gene leads to disproportionate overgrowth by an Igf2-independent mechanism. Proc. Natl. Acad. Sci. USA *100*, 8292–8297.

Ciemerych, M.A., and Sicinski, P. (2005). Cell cycle in mouse development. Oncogene *24*, 2877–2898.

Constancia, M., Kelsey, G., and Reik, W. (2004). Resourceful imprinting. Nature *432*, 53–57.

Cvetkovic, D., Pisarcik, D., Lee, C., Hamilton, T.C., and Abdollahi, A. (2004). Altered expression and loss of heterozygosity of the LOT1 gene in ovarian cancer. Gynecol. Oncol. *95*, 449–455.

DeChiara, T.M., Efstratiadis, A., and Robertson, E.J. (1990). A growth-deficiency phenotype in heterozygous mice carrying an insulin-like growth factor II gene disrupted by targeting. Nature *345*, 78–80.

Delaval, K., and Feil, R. (2004). Epigenetic regulation of mammalian genomic imprinting. Curr. Opin. Genet. Dev. *14*, 188–195.

Fraser, A.G., and Marcotte, E.M. (2004). Development through the eyes of functional genomics. Curr. Opin. Genet. Dev. *14*, 336–342.

Gardner, R.J., Mackay, D.J., Mungall, A.J., Polychronakos, C., Siebert, R., Shield, J.P., Temple, I.K., and Robinson, D.O. (2000). An imprinted locus associated with transient neonatal diabetes mellitus. Hum. Mol. Genet. *9*, 589–596.

Hoffmann, A., Ciani, E., Boeckardt, J., Holsboer, F., Journot, L., and Spengler, D. (2003). Transcriptional activities of the zinc finger protein Zac are differentially controlled by DNA binding. Mol. Cell. Biol. *23*, 988–1003.

Holm, T.M., Jackson-Grusby, L., Brambrink, T., Yamada, Y., Rideout, W.M., III, and Jaenisch, R. (2005). Global loss of imprinting leads to widespread tumorigenesis in adult mice. Cancer Cell *8*, 275–285.

Huang, S.M., and Stallcup, M.R. (2000). Mouse Zac1, a transcriptional coactivator and repressor for nuclear receptors. Mol. Cell. Biol. *20*, 1855–1867.

Huang, S.M., Schonthal, A.H., and Stallcup, M.R. (2001). Enhancement of p53-dependent gene activation by the transcriptional coactivator Zac1. Oncogene *20*, 2134–2143.

Kamiya, M., Judson, H., Okazaki, Y., Kusakabe, M., Muramatsu, M., Takada, S., Takagi, N., Arima, T., Wake, N., Kamimura, K., et al. (2000). The cell cycle control gene ZAC/PLAGL1 is imprinted—a strong candidate gene for transient neonatal diabetes. Hum. Mol. Genet. *9*, 453–460.

Kim, S.K., Lund, J., Kiraly, M., Duke, K., Jiang, M., Stuart, J.M., Eizinger, A., Wylie, B.N., and Davidson, G.S. (2001). A gene expression map for *Caenorhabditis elegans*. Science *293*, 2087–2092.

Kouskouti, A., Scheer, E., Staub, A., Tora, L., and Talianidis, I. (2004). Gene-specific modulation of TAF10 function by SET9-mediated methylation. Mol. Cell *14*, 175–182.

Koy, S., Hauses, M., Appelt, H., Friedrich, K., Schackert, H.K., and Eckelt, U. (2004). Loss of expression of ZAC/LOT1 in squamous cell carcinomas of head and neck. Head Neck *26*, 338–344.

Lee, H.K., Hsu, A.K., Sajdak, J., Qin, J., and Pavlidis, P. (2004a). Coexpression analysis of human genes across many microarray data sets. Genome Res. *14*, 1085–1094.

Lee, I., Date, S.V., Adai, A.T., and Marcotte, E.M. (2004b). A probabilistic functional network of yeast genes. Science *306*, 1555–1558.

Lefebvre, L., Viville, S., Barton, S.C., Ishino, F., Keverne, E.B., and Surani, M.A. (1998). Abnormal maternal behaviour and growth retardation associated with loss of the imprinted gene Mest. Nat. Genet. *20*, 163–169.

Leighton, P.A., Saam, J.R., Ingram, R.S., Stewart, C.L., and Tilghman, S.M. (1995). An enhancer deletion affects both H19 and Igf2 expression. Genes Dev. *9*, 2079–2089.

Li, L., Keverne, E.B., Aparicio, S.A., Ishino, F., Barton, S.C., and Surani, M.A. (1999). Regulation of maternal behavior and offspring growth by paternally expressed Peg3. Science *284*, 330–333.

Long, L., and Spear, B.T. (2004). FoxA proteins regulate H19 endoderm enhancer E1 and exhibit developmental changes in enhancer binding in vivo. Mol. Cell. Biol. *24*, 9601–9609.

Ma, D., Shield, J.P., Dean, W., Leclerc, I., Knauf, C., Burcelin, R.R., Rutter, G.A., and Kelsey, G. (2004). Impaired glucose homeostasis in transgenic mice expressing the human transient neonatal diabetes mellitus locus, TNDM. J. Clin. Invest. *114*, 339–348.

McGrath, J., and Solter, D. (1981). Completion of mouse embryogenesis requires both the maternal and paternal genomes. Cell *37*, 179–183.

Moon, Y.S., Smas, C.M., Lee, K., Villena, J.A., Kim, K.H., Yun, E.J., and Sul, H.S. (2002). Mice lacking paternally expressed Pref-1/Dlk1 display growth retardation and accelerated adiposity. Mol. Cell. Biol. *22*, 5585–5592.

Moore, J.H. (2005). A global view of epistasis. Nat. Genet. *37*, 13–14.

Moore, T., and Haig, D. (1991). Genomic imprinting in mammalian development: a parental tug-of-war. Trends Genet. *7*, 45–49.

Murrell, A., Heeson, S., and Reik, W. (2004). Interaction between differentially methylated regions partitions the imprinted genes Igf2 and H19 into parent-specific chromatin loops. Nat. Genet. *36*, 889–893.

Ohlsson, R. (2004). Loss of IGF2 imprinting: mechanisms and consequences. Novartis Found. Symp. *262*, 108–121.

Pagotto, U., Arzberger, T., Theodoropoulou, M., Grubler, Y., Pantaloni, C., Saeger, W., Losa, M., Journot, L., Stalla, G.K., and Spengler, D. (2000). The expression of the antiproliferative gene ZAC is lost or highly reduced in nonfunctioning pituitary adenomas. Cancer Res. *60*, 6794–6799.

Piras, G., El Kharroubi, A., Kozlov, S., Escalante-Alcalde, D., Hernandez, L., Copeland, N.G., Gilbert, D.J., Jenkins, N.A., and Stewart, C.L. (2000). Zac1 (Lot1), a potential tumor suppressor gene, and the gene for epsilon-sarcoglycan are maternally imprinted genes: identification by a subtractive screen of novel uniparental fibroblast lines. Mol. Cell. Biol. *20*, 3308–3315.

Plagge, A., Gordon, E., Dean, W., Boiani, R., Cinti, S., Peters, J., and Kelsey, G. (2004). The imprinted signaling protein XL alpha s is required for postnatal adaptation to feeding. Nat. Genet. *36*, 818–826.

Reik, W., and Lewis, A. (2005). Co-evolution of X-chromosome inactivation and imprinting in mammals. Nat. Rev. Genet. *6*, 403–410.

Reik, W., Constancia, M., Fowden, A., Anderson, N., Dean, W., Ferguson-Smith, A., Tycko, B., and Sibley, C. (2003). Regulation of supply and demand for maternal nutrients in mammals by imprinted genes. J. Physiol. *547*, 35–44.

Rozenfeld-Granot, G., Krishnamurthy, J., Kannan, K., Toren, A., Amariglio, N., Givol, D., and Rechavi, G. (2002). A positive feedback mechanism in the transcriptional activation of Apaf-1 by p53 and the coactivator Zac-1. Oncogene *21*, 1469–1476.

Segre, D., Deluna, A., Church, G.M., and Kishony, R. (2005). Modular epistasis in yeast metabolism. Nat. Genet. *37*, 77–83.

Siegal, M.L., and Bergman, A. (2002). Waddington's canalization revisited: developmental stability and evolution. Proc. Natl. Acad. Sci. USA *99*, 10528–10532.

Spengler, D., Villalba, M., Hoffmann, A., Pantaloni, C., Houssami, S., Bockaert, J., and Journot, L. (1997). Regulation of apoptosis and cell cycle arrest by Zac1, a novel zinc finger protein expressed in the pituitary gland and the brain. EMBO J. *16*, 2814–2825.

Surani, M.A., Barton, S.C., and Norris, M.L. (1984). Development of reconstituted mouse eggs suggests imprinting of the genome during gametogenesis. Nature *308*, 548–550.

Takahashi, K., Nakayama, K., and Nakayama, K. (2000). Mice lacking a CDK inhibitor, p57Kip2, exhibit skeletal abnormalities and growth retardation. J. Biochem. (Tokyo) *127*, 73–83.

Tsuda, T., Markova, D., Wang, H., Evangelisti, L., Pan, T.C., and Chu, M.L. (2004). Zinc finger protein Zac1 is expressed in chondrogenic sites of the mouse. Dev. Dyn. *229*, 340–348.

Tycko, B., and Morison, I.M. (2002). Physiological functions of imprinted genes. J. Cell. Physiol. *192*, 245–258.

Valente, T., and Auladell, C. (2001). Expression pattern of Zac1 mouse gene, a new zinc-finger protein that regulates apoptosis and cellular cycle arrest, in both adult brain and along development. Mech. Dev. *108*, 207–211.

Vandesompele, J., De Preter, K., Pattyn, F., Poppe, B., Van Roy, N., De Paepe, A., and Speleman, F. (2002). Accurate normalization of real-time quantitative RT-PCR data by geometric averaging of multiple internal control genes. Genome Biol. *3*, RESEARCH0034.

Varrault, A., Ciani, E., Apiou, F., Bilanges, B., Hoffmann, A., Pantaloni, C., Bockaert, J., Spengler, D., and Journot, L. (1998). hZAC encodes a zinc finger protein with antiproliferative properties and maps to a chromosomal region frequently lost in cancer. Proc. Natl. Acad. Sci. USA *95*, 8835–8840.

Varrault, A., Bilanges, B., Mackay, D.J., Basyuk, E., Ahr, B., Fernandez, C., Robinson, D.O., Bockaert, J., and Journot, L. (2001). Characterization of the methylation-sensitive promoter of the imprinted ZAC gene supports its role in transient neonatal diabetes mellitus. J. Biol. Chem. *276*, 18653–18656.

Verona, R.I., Mann, M.R., and Bartolomei, M.S. (2003). Genomic imprinting: intricacies of epigenetic regulation in clusters. Annu. Rev. Cell Dev. Biol. *19*, 237–259.

Vivian, J.L., Olson, E.N., and Klein, W.H. (2000). Thoracic skeletal defects in myogenin- and MRF4-deficient mice correlate with early

defects in myotome and intercostal musculature. Dev. Biol. *224*, 29–41.

Wagner, A. (2000). Robustness against mutations in genetic networks of yeast. Nat. Genet. *24*, 355–361.

Wang, Z.Q., Fung, M.R., Barlow, D.P., and Wagner, E.F. (1994). Regulation of embryonic growth and lysosomal targeting by the imprinted Igf2/Mpr gene. Nature *372*, 464–467.

Wilkins, J.F., and Haig, D. (2003). What good is genomic imprinting: the function of parent-specific gene expression. Nat. Rev. Genet. *4*, 359–368.

Wu, L.F., Hughes, T.R., Davierwala, A.P., Robinson, M.D., Stoughton, R., and Altschuler, S.J. (2002). Large-scale prediction of *Saccharomyces cerevisiae* gene function using overlapping transcriptional clusters. Nat. Genet. *31*, 255–265.

Yoo-Warren, H., Pachnis, V., Ingram, R.S., and Tilghman, S.M. (1988). Two regulatory domains flank the mouse H19 gene. Mol. Cell. Biol. *8*, 4707–4715.

Zhang, W., Morris, Q.D., Chang, R., Shai, O., Bakowski, M.A., Mitsakakis, N., Mohammad, N., Robinson, M.D., Zirngibl, R., Somogyi, E., et al. (2004). The functional landscape of mouse gene expression. J. Biol. *3*, 21.